Research article

JGS
Journal of the Geological Society

https://doi.org/10.1144/jgs2024-269 | Vol. 182 | 2025 | jgs2024-269

Microbially mediated carbonates in the Mesoproterozoic Stoer Group of NW Scotland; earliest evidence of life in Britain?

Peter Gutteridge

Department of Earth and Environmental Sciences, The University of Manchester, Oxford Road, Manchester M13 9PL, UK
0000-0001-7094-5673
Correspondence: peter.gutteridgedr@outlook.com

Abstract: Lake margin and associated facies in the Mesoproterozoic Stoer Group of NW Scotland contain laminated carbonate structures and sediment surface textures. The former are reinterpreted as microbial stromatolites based on the combined evidence of constructional depositional relief, binding of sediment to support subvertical and overhanging layers and the presence of microbially mediated carbonate fabrics. Stromatolites range from domical structures a few centimetres across with a depositional relief of a few centimetres deposited in very shallow water in lake margin settings to biohermal structures several metres thick and several tens of metres in lateral extent that occur in lake margin settings and drape fan-delta lobes that prograded into lakes. Sediment surface textures are represented by laterally linked domes on mudstone bedding planes, desiccated carbonate sheets and mudstone coatings on fluvial surfaces and fan-delta lobes in conglomeratic facies. The biological involvement in the formation of sediment surface textures is not proven. The formation of sediment surface textures as opposed to stromatolites may reflect variations in the degree of carbonate saturation of the groundwater or differing communities of microbial species. Dissolved sulfate may have been supplied by weathering of sulfides, whereas carbonate may have been supplied by semi-arid weathering of Scourian dykes. Marine–freshwater mixing zones are another possible source of sulfates and carbonates.

Received 29 November 2024; **revised** 14 April 2025; **accepted** 25 April 2025

The Stoer Group is a succession of unmetamorphosed Mesoproterozoic red beds up to 2.5 km thick in NW Scotland between 1200 and 1100 Ma old (Fig. 1a and b; Turnbull *et al.* 1996; Stewart 2002; Amor *et al.* 2008; Parnell *et al.* 2011). It contains well-documented examples of planar and domical structures ranging from a few centimetres to several tens of metres in size that are composed of laminated carbonate, siltstone and mudstone that occur in alluvial, lacustrine and possible marine-influenced settings (Upfold 1984; Prave 2002; Stewart 2002; Brasier *et al.* 2017, 2019; Stüeken *et al.* 2017). These structures have been referred to as pseudostromatolites because their origin has previously been attributed to abiogenic processes including desiccation, replacement of evaporites, dewatering and as clastic structures in which the carbonate component was reworked from older metamorphic rocks (e.g. Stewart 2002; Brasier *et al.* 2017, 2019).

Sediment surface textures are often also present in sediments associated with these laminated carbonate structures. These include wrinkle structures on fine sandstone beds, patches of sand on bedding planes in mud rock that have irregular or ragged margins and rod-shaped intraclasts of mud rock in ripple troughs interpreted as rolled mats; the latter have been referred to the pseudofossil *Manchuriophycus* (Prave 2002; Brasier *et al.* 2017, 2019; McMahon and Davies 2018). The origin of these features is uncertain but has been attributed to microbially induced sedimentary structures implying surficial binding of the sediment by microbial mats; however, the biological origins of these structures have not been conclusively proven (e.g. Davies *et al.* 2016).

The aims of this paper are to provide an interpretation of the sedimentological context in which the laminated carbonate structures and sediment surface textures occur and to re-evaluate their possible origins. This includes a comparison of the carbonate microfabric with other known examples of microbial carbonates and integrates recent developments in our understanding of the roles of microbial activity in carbonate production (e.g. Noffke 2009; Bosence *et al.* 2015; Fedorchuk *et al.* 2016; Kah and Bartley 2021). Selected sections were logged to focus on the sedimentological context of the sediment surface textures and laminated carbonate structures in the Clachtoll Formation at Clachtoll and the Poll a'Mhuilt Member of the Bay of Stoer Formation at the Bay of Stoer and Enard Bay (Fig. 1a and b). Plane-polarized light and cathodoluminescence (CL) images were obtained by a CITL cold cathode luminoscope Mk5-1 and a Nikon Eclipse LV100 microscope with an electron beam operating at 410–420 µA and 10–11 kV with a chamber pressure of 0.003 mbar. Polished thin sections were prepared from a loose block collected at Enard Bay.

Stratigraphic summary

The stratigraphy of the Stoer Group is summarized by Figure 1b and c. The Clachtoll Formation onlaps the Lewisian palaeosurface with incised palaeovalleys infilled by alluvial fan and rockfall deposits (Stewart 2002; Killingback *et al.* 2021). These pass laterally into a muddy flood basin facies with single or multiple fluvial channels and lakes in interchannel areas (Stewart 2002; Ielpi *et al.* 2016; Valenza *et al.* 2019).

The overlying Bay of Stoer Formation consists of sandstone with minor shale deposited as fluvial channels on floodplains (Stewart 2002). The upper part of the Bay of Stoer Formation comprises two Members: the Stac Fada Member, interpreted as a meteorite impact breccia by Amor *et al.* (2008), and the Poll a'Mhuilt Member. At the Bay of Stoer, the Poll a'Mhuilt Member consists of red organic-rich mudstone with sandstone and carbonate intervals. Stewart and Parker (1979), Stewart (2002) and Parnell *et al.* (2015) suggested that this represents an evaporitic lake; however, Stüeken *et al.* (2017) proposed that this interval was influenced by marine water. Upfold (1984) identified planar, mammillated and tufted mats in the

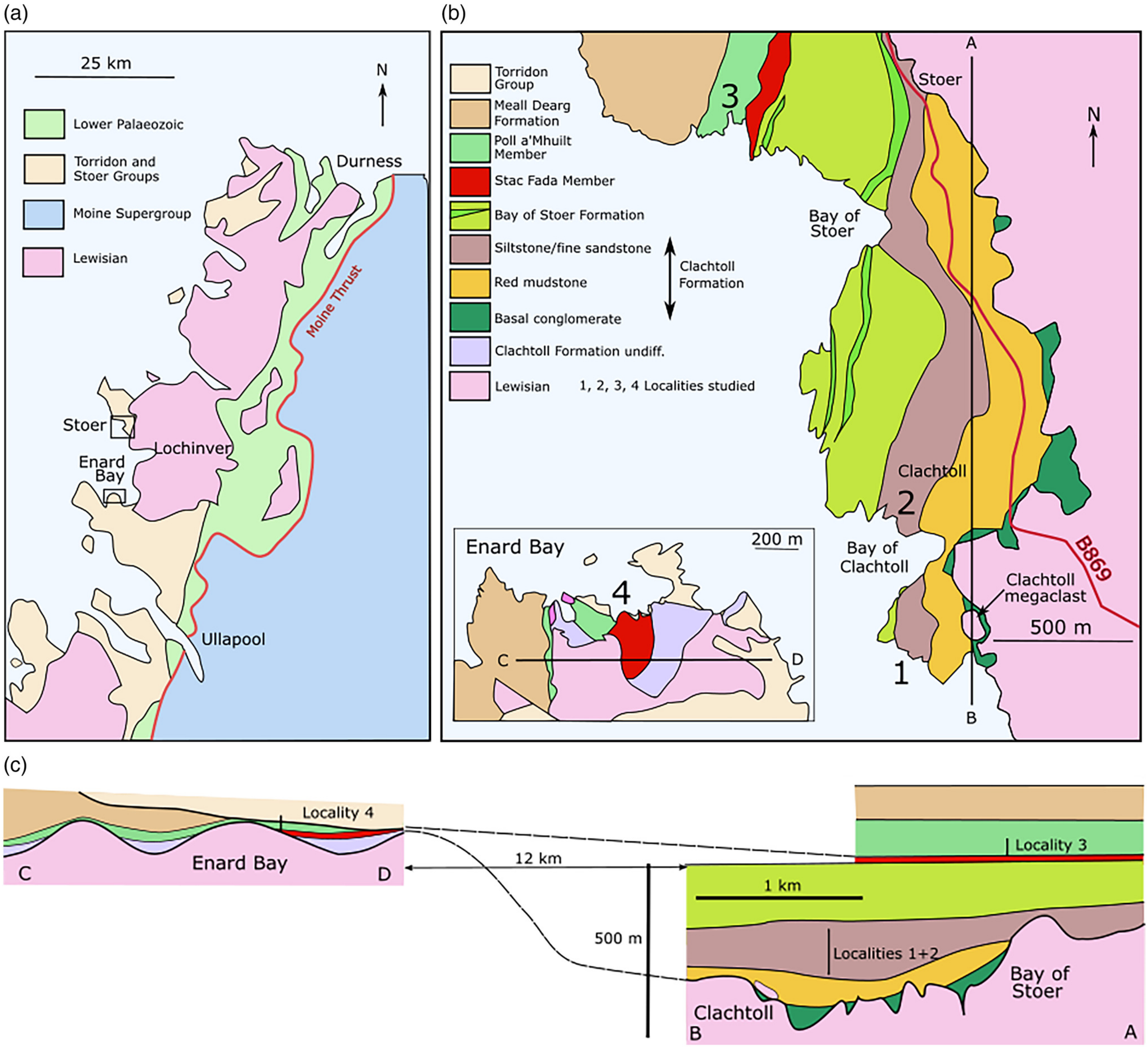

Fig. 1. (**a**) General location of the Stoer Group outcrop and study area in NW Scotland. (**b**) Localities studied. Bay of Stoer Formation consists mainly of fluvial sandstone (pale green) interbedded with shale intervals (dark green). The Bay of Stoer Formation also includes the Stac Fada and Poll a'Mhuilt Members. Locality 1 [NC03802665]; locality 2 [NC03852710]; locality 3 [NC03352860]; locality 4 [NC02861462]. (**c**) Simplified stratigraphic summary of the Stoer Group showing relationship between the two areas. Vertical and horizontal scales are the same for each section. Source: (b) Clachtoll megaclast from Killingback *et al.* (2021); Enard Bay inset adapted from Goodenough and Krabbendam (2011); (c) adapted from Gracie and Stewart (1967), Stewart (2002) and Goodenough and Krabbendam (2011).

Poll A'Mhuilt Member, which he interpreted as microbial stromatolites. At Enard Bay, the Poll a'Mhuilt Member comprises alluvial breccio-conglomerates shed from local palaeohills in the Lewisian land surface that pass laterally into lacustrine mudstone with carbonates (Gracie and Stewart 1967; Stewart 2002). The Meall Dearg Formation consists of cross-bedded fluvial sandstone with some aeolian facies (McMahon and Davies 2018).

Description of selected sections

The two following sections provide a detailed description and interpretation of the sedimentology, carbonate microfabrics and depositional environments of the sections in which the laminated carbonate structures and sediment surface textures are found. An overview of the possible origins of these structures will be presented in the discussion section.

Clachtoll Formation, Clachtoll, localities 1 and 2

The logged sections are 1.5–2 m thick intervals of laminated sandstone, siltstone and mudstone that are interbedded with structureless fine muddy sandstone some 8–15 m thick (Fig. 2). These intervals consist mainly of muddy siltstone with planar laminated fine to medium sand a few millimetres to centimetres in thickness and carbonate sheets composed of calcite microspar a few millimetres in thickness (Fig. 3a). Occasional interbedded layers of erosionally based fine to medium sandstone with granule- and fine pebble-sized tabular clasts of red mudstone are also present (Fig. 3b). Some of the sand laminae have been cut by structures injected with sand and silt, and some chaotic intervals with convolute lamination are present. Isolated symmetrical ripples of fine sandstone with cross-bedding up to 2 cm thick and wavelengths of 5–10 cm are present at a number of horizons and are often exposed on bedding planes (Fig. 3c). Lenses of fine sand,

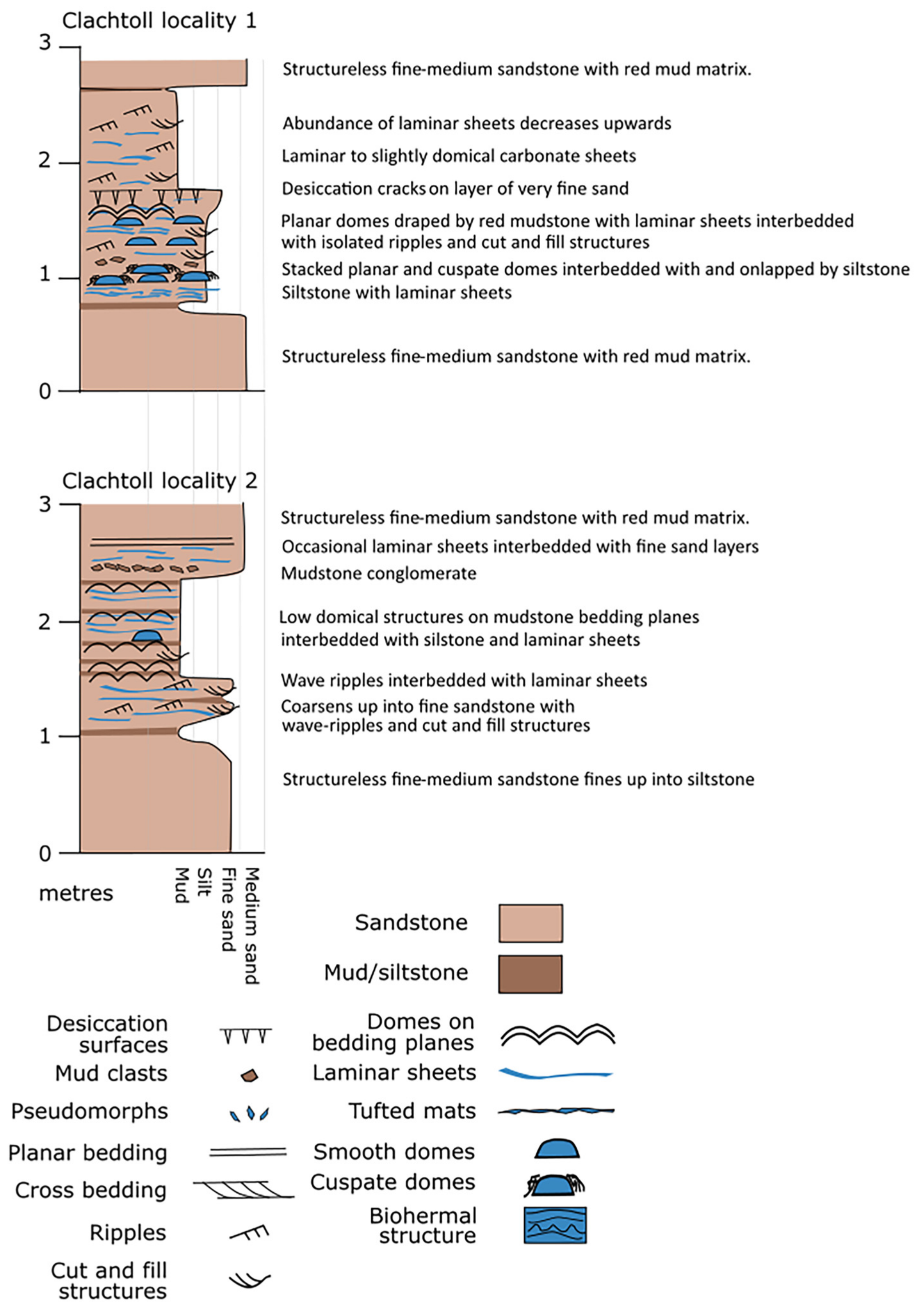

Fig. 2. Sedimentological logs of selected sections in the Clachtoll Formation at Clachtoll, locality 1 [NC03652685]; locality 2 [NC03752720]. Key also refers to Figure 5.

sometimes showing bimodal trough-bedding, infill channel-like structures with scoured basal surfaces a few centimetres across (Fig. 3d). Many of the isolated ripples and sand-filled cut and fill structures are deformed and have foundered into the underlying siltstone and mudstone (Fig. 3e). Mud- and siltstone layers are often cut by a polygonal network of subvertical cracks infilled by fine sand that die out downwards; some of these fractures are sinuous (Fig. 3f). Bedding plane exposures of carbonate sheets often have a network of polygonal ridges but with no associated downward penetrating fractures (Fig. 3g). Some mudstone and siltstone bedding planes display low-relief laterally linked domes that are symmetrical to slightly elongate structures up to 20 cm across with a relief of a few millimetres to centimetres (Fig. 3h). The troughs between domes contain stringers of silt- and very fine sandstone that onlap the margins of the domes.

Domical structures made up of sub-parallel, planar to undulatory carbonate layers occur in this facies association (Fig. 4a and b). The carbonate laminae show two fabric types: layers of equant calcite microspar and layers composed of calcite plates that have a sub-parallel to irregular alignment that imparts a ‘crinkly’ fabric to the layering (Fig. 4b and c). Both types of carbonate laminae are up to a few millimetres thick and alternate with sub-millimetre thick partings of mudstone and siltstone. The domes show two morphological types, as follows.

Smooth domes are equant to slightly elongate to symmetrical structures with lateral dimensions of 5–20 cm between 1 and 5–10 cm thick with flat sub-parallel bases and tops with margins whose dip varies from 30° to vertical (Fig. 4a and b). Most smooth domes are isolated structures that are interbedded with and onlapped by planar and ripple-laminated siltstone and fine sandstone (Fig. 4a and b). Carbonate layers within the domes mimic the external form of the dome, often thinning towards the edges of domes. Smooth domes often contain intervals of the microspar fabric alternating with the crinkly fabric (Fig. 4a and b) and the margins of some domes consist of the crinkly fabric whereas the dome interior consists of microspar layers. Clastic mudstone layers also alternate with the microspar and crinkly layers. Smooth domes show alternating offlapping and back-stepping forms (Fig. 4b).

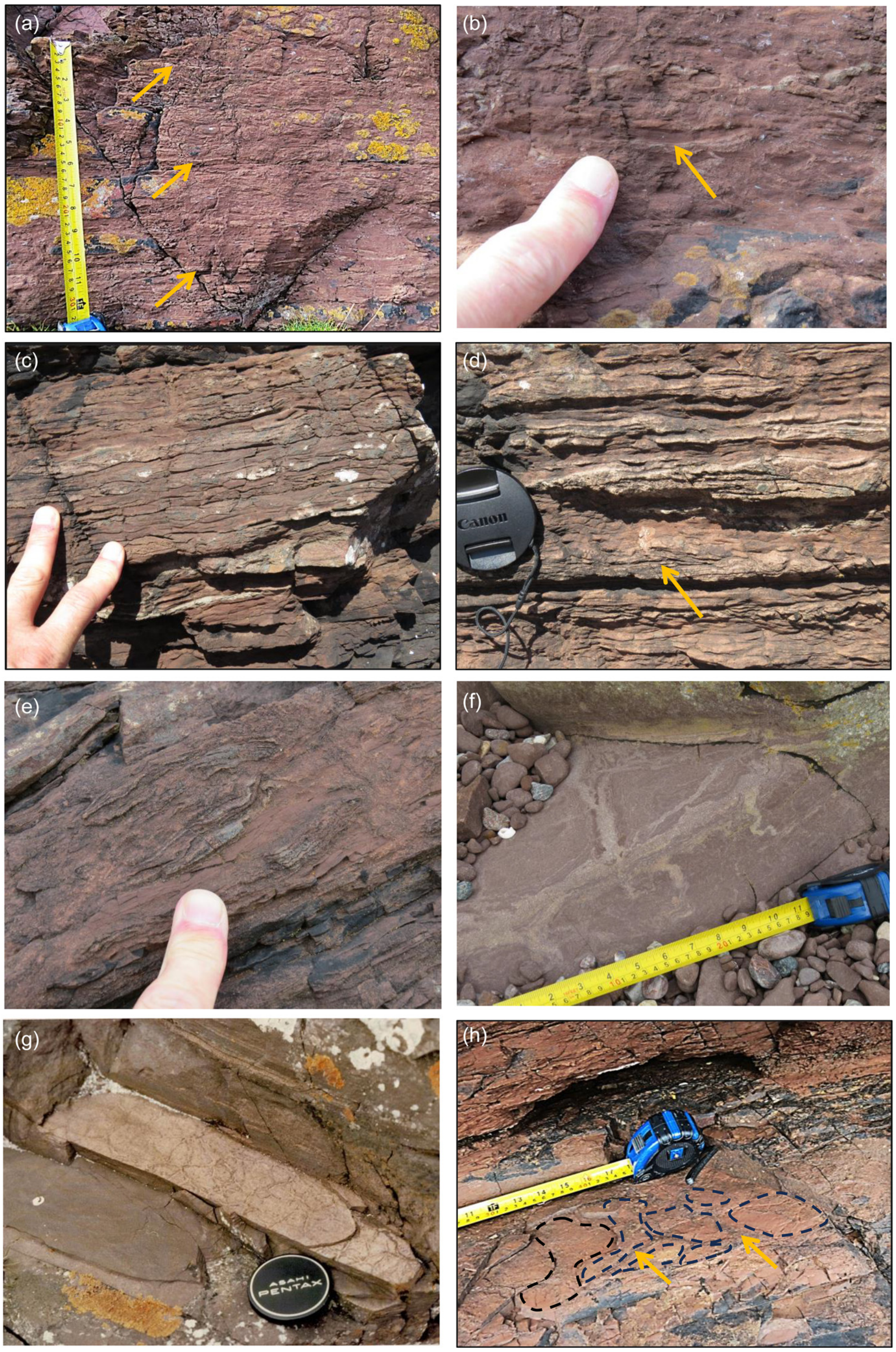

Fig. 3. Clachtoll Member, Clachtoll, localities 1 and 2. (**a**) Wide vertical spacing of laminar sheets (yellow arrows) interbedded with siltstone and thinly layered very fine sandstone with occasional isolated ripples. Locality 2. (**b**) Fine to medium sandstone with granule- to pebble-sized tabular clasts of red mudstone (arrow). Locality 2. (**c**) Laminated mudstone with symmetrical ripples and occasional channel-like bodies with scoured bases infilled by trough-bedded fine sandstone. Locality 1. (**d**) Detail of cut and fill structures in silty mudstone infilled by ripple-bedded fine sandstone and occasional bimodal trough cross-bedding (yellow arrow). Locality 1. Lens cap 5 cm in diameter. Locality 1. (**e**) Foundered fine sand-sized isolated ripple showing recumbent folding and overturned bedding surrounded by dewatered siltstone. Locality 1. (**f**) Polygonal fractures in mudstone infilled by fine sand; fractures in vertical section are sinuous. Locality 2. (**g**) Carbonate sheet with polygonal network of ridges; it should be noted that there are no corresponding subvertical fractures associated with these ridges. Lens cap is 49 mm across. Locality 2. (**h**) Bedding plane in mudstone showing low-relief domes (outlined) with stringers of darker reddish brown very fine sand and silt preserved between the domes (yellow arrows). Locality 1.

Cuspate domes have similar dimensions to smooth domes, but the carbonate component is made up of the crinkly carbonate fabric (Fig. 4c). The bases of cuspate domes are planar to undulatory carbonate layers developing into more pronounced undulations; the upper parts of cuspate domes display irregular asymmetrical upward-projecting cuspate forms (Fig. 4c). Some clastic-rich layers and grains are included with the cuspate domes. The morphology of the internal layering also mimics the external form of the dome.

Poll a'Mhuilt Member, Bay of Stoer, locality 3

The basal 14.6 m of the Poll a'Mhuilt Member, including carbonate-bearing units A to C of Stewart (2002, p. 68), was logged from the top of the Stac Fada Member (Fig. 5).

The lowermost 4.0 m (interval 1, Fig. 5) consists of beds 0.1–0.5 m thick of structureless moderately sorted fine to medium sandstone sand-sized grains and granule-sized tabular clasts of red mudstone alternating with thin shale beds. Sandstone beds are ungraded with non-channelized bases. An interbedded package up to 1.0 m in thickness of fine sandstone, siltstone and mudstone with thin carbonate layers is present (Fig. 5). This comprises planar and ripple-bedded fine sandstone interbedded with siltstone and mudstone. Bedding planes with linear to sinuous symmetrical ripples are present (Fig. 6a). Occasional bedding surfaces with laterally linked low-relief symmetrical domical structures occur in this interval. The individual domes are a few centimetres in lateral dimension and a few millimetres in relief (Fig. 6b, yellow arrow). Bedding surfaces penetrated by sand-filled polygonal desiccation fractures also occur in this interval (Fig. 6b, red arrow).

Planar to undulatory carbonate sheets 1–2 mm in thickness composed of microspar are also interbedded with the rippled and laminated sandstone and siltstone with occasional acicular and

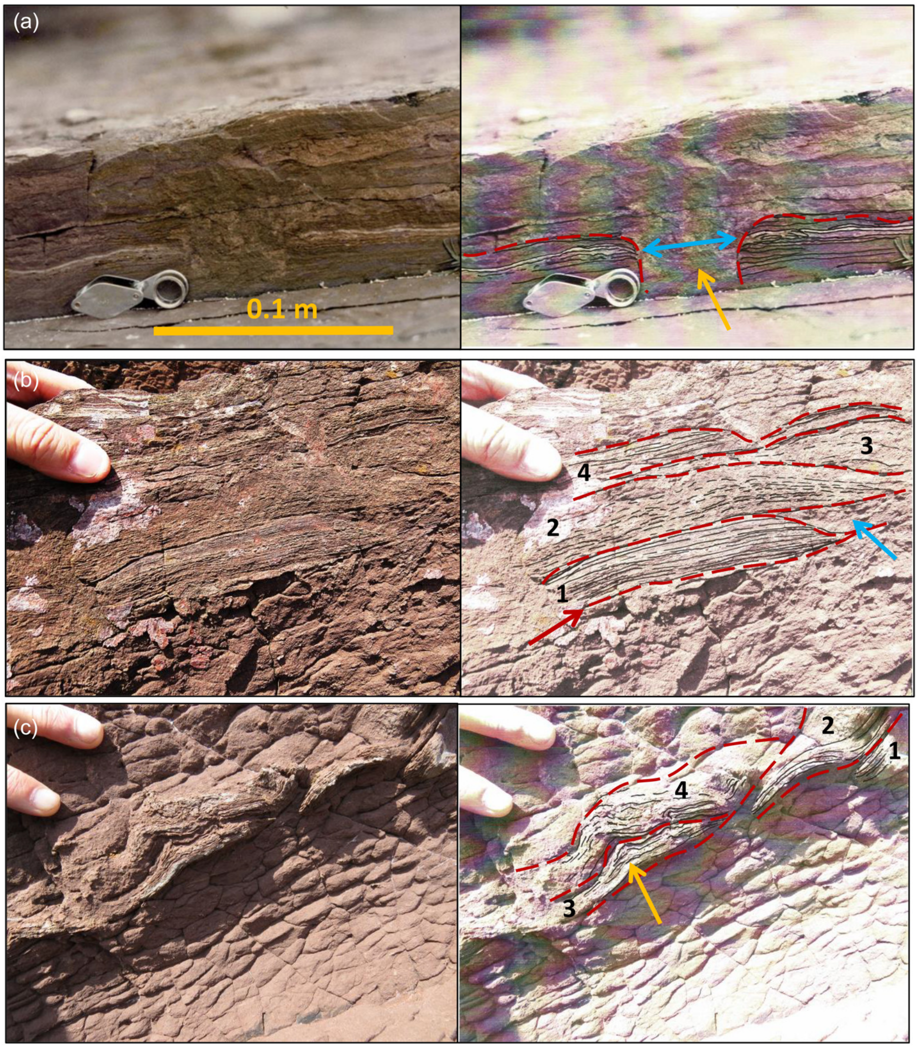

Fig. 4. (**a**) Adjacent isolated smooth domes with vertical margins separated by fine sandstone and siltstone (yellow arrow). Each dome comprises alternating planar uniform carbonate and siltstone layers with the development of discontinuous carbonate layers at the same level in each dome (blue arrow). (**b**) Smooth dome (1) with planar base overlying fine sandstone (red arrow). Internal microspar laminae are sub-parallel and dip towards the margins of the dome. The right-hand margin of Dome 1 is onlapped by lens-shaped package of fine silty sandstone (blue arrow). Dome 1 plus the lens of siltstone is then overgrown by Dome 2, which has a crinkly internal fabric. Dome 2 is then further overgrown by smaller offlapping isolated domes 3 and 4. (**c**) Cuspate dome with crinkly internal carbonate fabric that consists of small domes with planar to undulatory bases showing offlapping growth (domes 1 and 2). Dome 3 shows upward development of sharply 'folded' cusp (yellow arrow). Final form of dome (4) shows further development of upward projecting cusp.

chevron-shaped single crystal pseudomorphs infilled by carbonate in associated sediment. These carbonate sheets are mainly planar, but some clusters of microspar form upward-branching tuft-like and conical projections (Fig. 6c) forming elongate to equant low-relief domes a few millimetres to centimetres in height and 10–15 cm in wavelength that are onlapped by siltstone and fine sandstone (Fig. 6d). Upfold (1984) showed that the carbonate texture consists of uniform equant microspar. The topmost 0.5 m of interval 1 consists of ripple-bedded fine sandstone, siltstone and red mudstone interbedded with carbonate sheets composed of coarse equant microspar 0.5–1.0 mm in thickness (Fig. 6e). The carbonate sheets increase in frequency upwards to form a laminated carbonate structure comprising layers of equant microspar alternating with packages of the crinkly carbonate fabric described from Clachtoll Bay, locality 1 (Fig. 2). The internal structure consists of planar to slightly domical carbonate laminae with a sharp top overlain by a cross-bedded medium sandstone.

Interval 2 consists of planar bedded laminated siltstone interbedded with fine sandstone with some tufted carbonate sheets overlain by a laminated carbonate unit 0.6 m thick that sits in a sharp, channelized base (Fig. 5). Its internal structure consists of laterally continuous planar and domical millimetre-scale sheets of calcite microspar that form broad overlapping domical structures. The top of the carbonate unit is sharp.

Interval 3 consists of a planar bedded fine sandstone with occasional carbonate sheets that fines upwards into a laminated siltstone and mudstone with planar carbonate sheets that increase in frequency upwards, amalgamating into a laminated carbonate structure up to 2.0 m in thickness (Fig. 5). The lower part of the carbonate structure comprises planar laminations with some low-relief symmetrical domes (Fig. 6f). This culminates in a layer of smaller higher relief domes up to 0.2 m in lateral and vertical dimension (Fig. 6g). The upper part of the carbonate interval shows a series of broad overlapping symmetrical domes that develop on the layer of smaller domes (Fig. 6h). These are 0.5–1.9 m across with a vertical relief of between 0.2 and 0.3 m. The internal morphology of the carbonate laminae mimics the external form of the structures. The top of this carbonate interval is sharp with broad domical structures onlapped by medium to fine sandstone (Fig. 5).

Poll a'Mhuilt Member, Enard Bay, locality 4

Breccio-conglomerates form a series of tabular bodies 5–10 m in thickness that offlap the Lewisian basement. Some breccio-conglomerate bodies are dominated by pebble-sized conglomerates whereas other are dominated by coarser cobble- and boulder-sized clasts. The breccio-conglomerates comprise poorly sorted rounded to sub-angular, pebble- to cobble- and boulder-sized clasts of Lewisian material with a matrix of finer clasts and medium to very coarse sand-sized quartz grains (Fig. 7a–d). Coarse-grained cobble- and boulder-sized breccio-conglomerates tend to be very poorly stratified with very crudely developed grading (Fig. 7d and e), whereas finer-grained pebble conglomerates and pebbly sandstone tend to show better developed grading and stratification that is picked out by alignment, layering and imbrication of clasts. Individual layers can be distinguished by their sharp bases, contrasting clast angularity and abrupt upward increase of clast

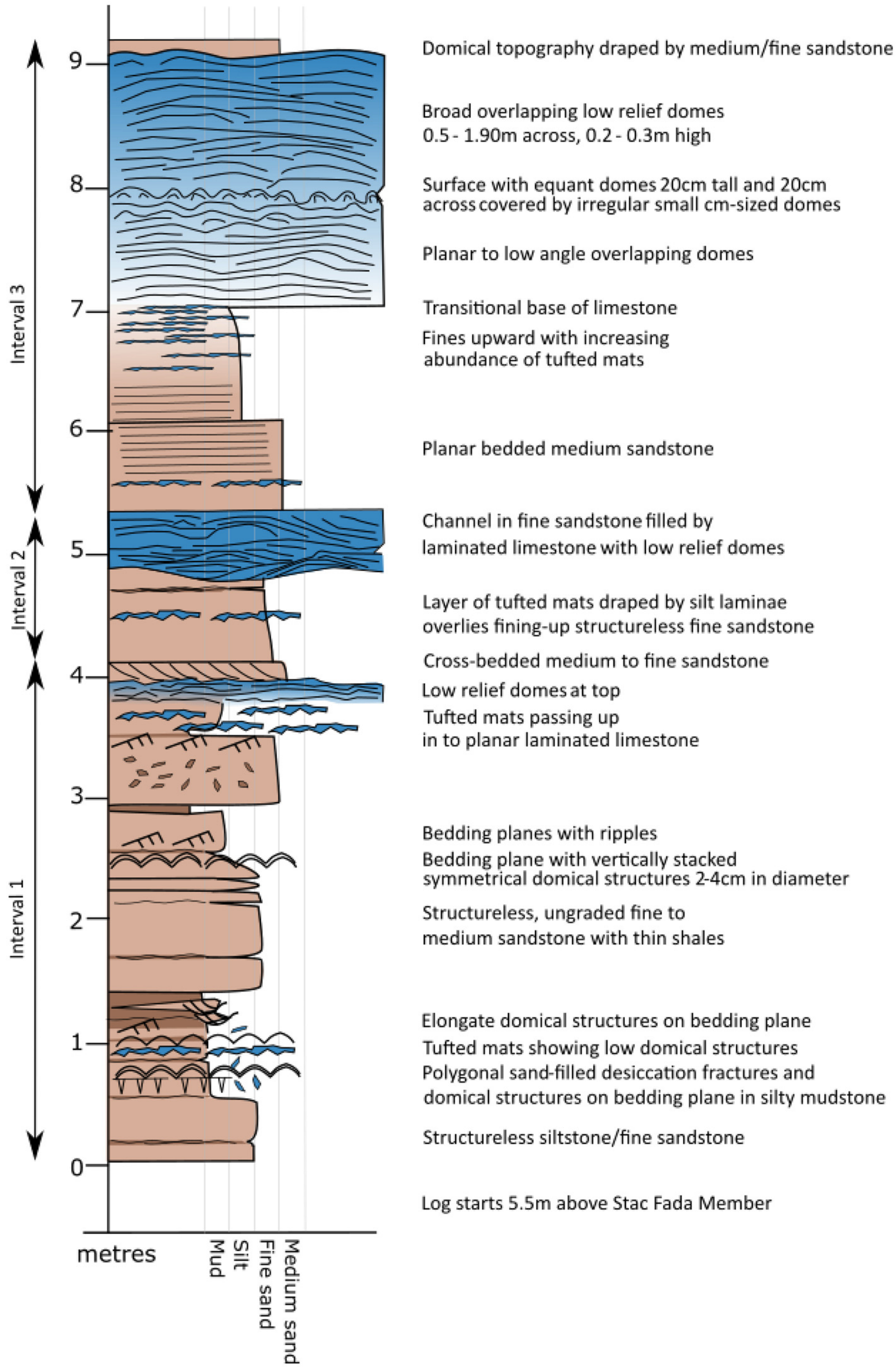

Fig. 5. Sedimentological log of the basal part of the Poll a'Mhuilt Member, Bay of Stoer locality 3 [NC03252855]. The key is shown in Figure 2.

size. Each of the tabular breccio-conglomeratic bodies terminates at a low-angle oblique clinoform surface (Fig. 7b and e).

Clasts in pebble-sized conglomerates have a red mudstone matrix that forms a coating of millimetre-thick undulatory mudstone laminae that wraps or drapes rounded pebble-sized clasts and surfaces but does not form coatings of individual clasts (Fig. 7a–c). Some clinoform surfaces within breccio-conglomeratic bodies have also been coated by the red mudstone (Fig. 7b). Mudstone coatings sometimes include centimetre-thick layers of moderately sorted, sub-angular to subrounded coarse sand-sized grains (Fig. 7c). These sand layers are often undulatory with sharp, occasional scoured bases and transitional tops. No desiccation features or any rip-up clasts of the red mudstone have been found.

Calcareous laminated red mudstone interfingers with and overlies the breccio-conglomerate bodies; in some places, it lies directly on the Lewisian palaeosurface (Fig. 7e). It forms a thick drape of clinoform surfaces at the termination of breccio-conglomerate bodies, thickening away to form a body of laminated calcareous mudstone several metres thick (Fig. 7e and f). The total thickness, lateral extent and the nature of the upper surface of the calcareous red mudstone is not known because it has been truncated by the unconformity at the base of the Diabaig Formation (Fig. 7f).

The large-scale structure of the calcareous red mudstone comprises numerous broad, symmetrical low-relief, overlapping convex-upward domical structures, up to 5–10 m across and 0.25–0.50 m in height (Fig. 7f–i). The internal carbonate layers tend to mimic the external form of these domical structures (Fig. 7g–i). Domical structures tend to be centred around individual cobbles and boulders forming smaller, higher relief domes that project upwards from the breccio-conglomerate layer (Fig. 7g). The carbonate and mudstone layers coating some clasts are subvertical to overhanging in attitude (Fig. 7g). These domes expanded beyond the initial clast,

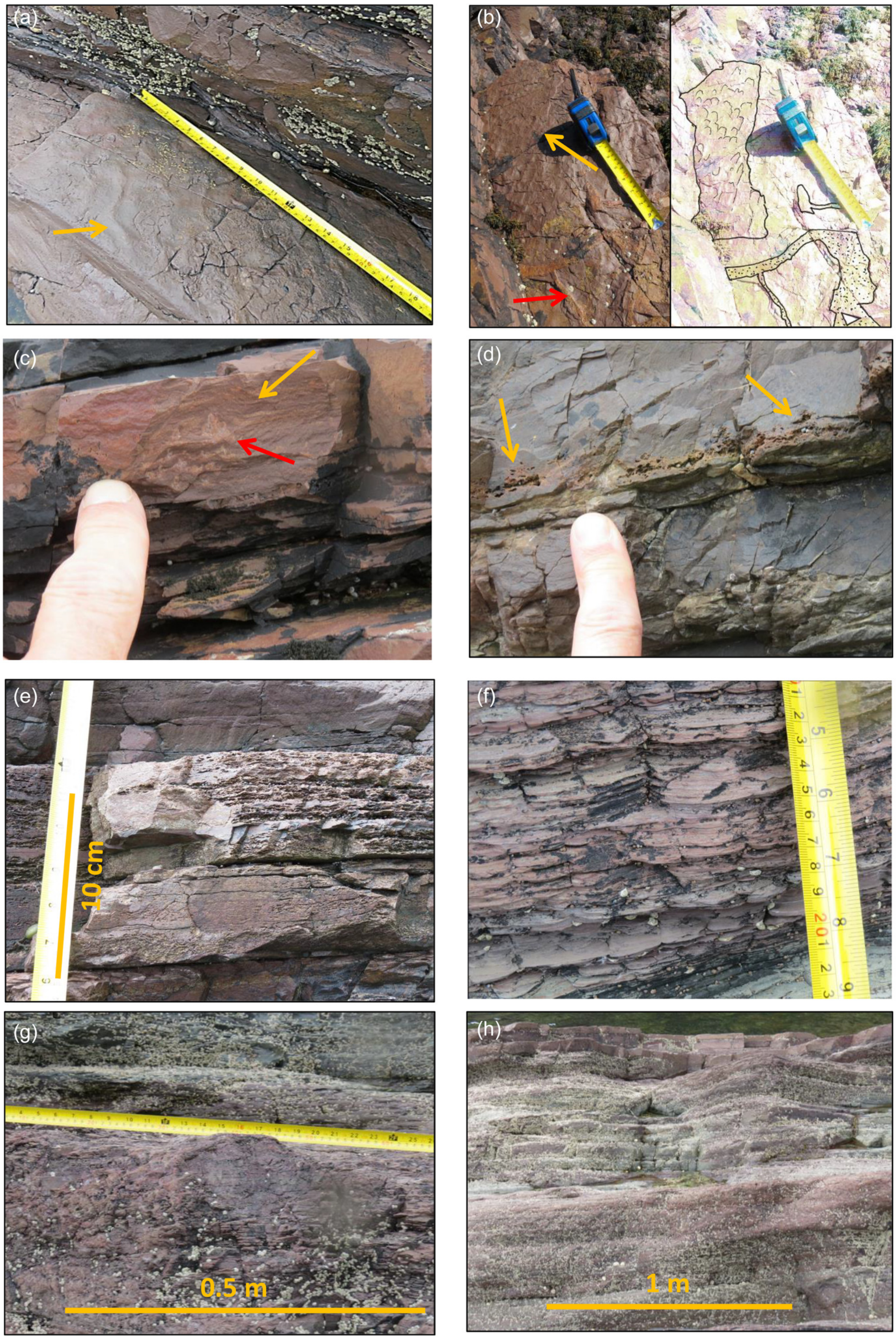

Fig. 6. Poll a'Mhuilt Member, Stoer Bay, locality 3. (**a**) Bedding plane in fine sandstone with mudstone drape showing intersecting ripple sinuous crests (arrow) interpreted as interference ripples. (**b**) Bedding plane in fine sandstone with mudstone showing laterally linked symmetrical domes (yellow arrow) with polygonal desiccation fractures infilled by paler fine sand (red arrow). (**c**) Carbonate layers composed of coarse microspar with intercrystal porosity showing tufted structure projecting into overlying mudstone. Poll a'Mhuilt Member, Bay of Stoer, locality 3. (**d**) Discontinuous carbonate sheets with minor intercrystal porosity interbedded with siltstone showing slight domical structure in overlying bedding plane (yellow arrow). (**e**) Stacked planar carbonate sheets passing transitionally upwards from laminated siltstone. (**f**) Transitional base of upper carbonate interval with layers of siltstone interlaminated with increasing upward abundance of fine calcite microspar layers. (**g**) Lower part of biohermal structure with planar to low-relief symmetrical domes capped by layer of smaller higher relief irregular domes up to 0.2 m (at level of tape measure). (**h**) Upper part of upper biohermal carbonate interval showing transition from broad low-relief domes to smaller, higher relief domes at top of carbonate interval.

becoming much broader and of lower relief, and overgrow any adjacent domical structures (Fig. 7g–i). Much of the upper surface of the calcareous red mudstone comprises numerous low-relief overlapping domes several tens of metres in lateral extent and between 1.5 and 2.0 m in thickness (Fig. 7h and i). No desiccation structures were found in the laminated red mudstone.

The laminated calcareous mudstone comprises millimetre- to centimetre-thick layers of red mudstone alternating with irregular, elongate to equant-shaped calcite bodies concentrated in layers (Fig. 8a and b). The larger irregular carbonate bodies are up to 3 cm in length and 2 cm in thickness; their bases are flat to slightly convex-down, whereas the upper surfaces tend to have low-relief convex-upward forms (Fig. 8b). The larger carbonate bodies are surrounded by smaller equant and tabular-shaped bodies that appear to be fragments of the larger bodies (Fig. 8a and b). Some of the latter show a preferential sub-parallel alignment (Fig. 8e and f). The matrix consists of semi-opaque siliciclastic red mudstone with scattered silt- and fine sand-sized sub-angular detrital quartz and feldspar grains. It is non-luminescent and occurs as pervasive wispy microstylolitic pressure dissolution seams at the margins of the carbonate bodies, sometimes truncating their internal fabric (Fig. 8c and d).

The carbonate bodies are composed of two microfabrics (Fig. 8e and f), as follows.

- Clotted micrite: these are dense to dispersed aggregates of rounded to irregular peloids up to 500 μm in size composed of homogeneous micrite that has a mottled to speckly moderate yellowish orange luminescence (Figs 8e and 9). The pore space between the clotted micrite is infilled by

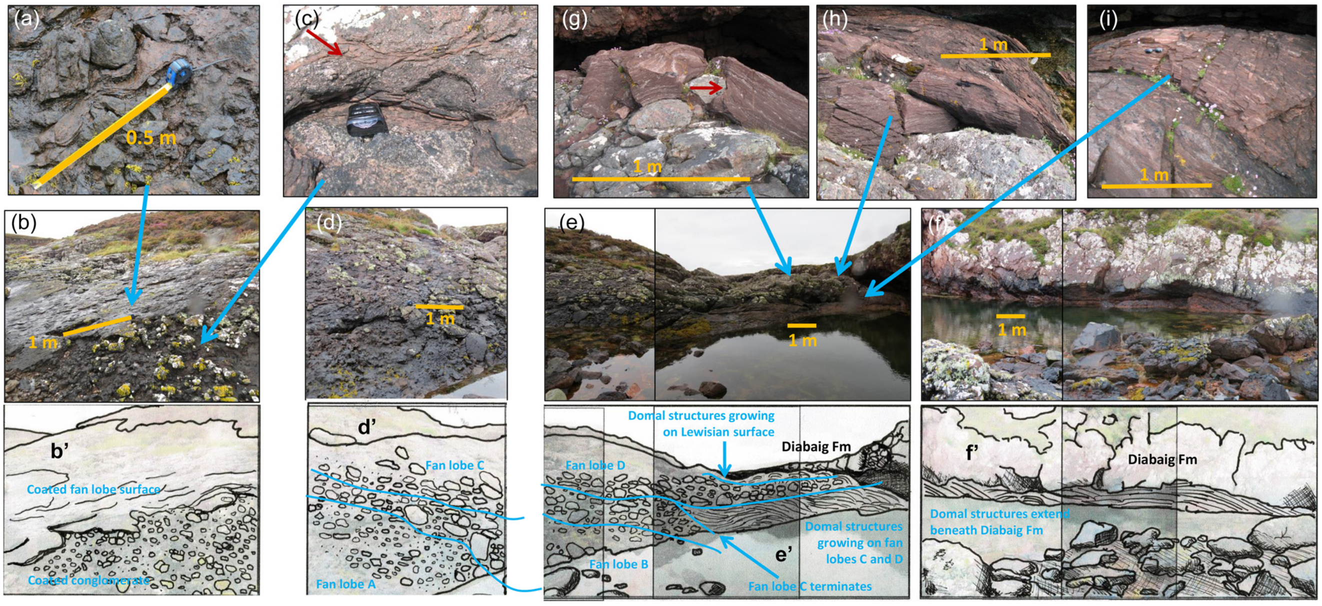

Fig. 7. (**a**–**i**) Poll a'Mhuilt Member, Enard Bay, locality 4 [NC02851460]. (**b**), (**d**), (**e**), (**f**) composite panorama of the outcrop; (**b**′), (**d**′), (**e**′), (**f**′) field sketches. (**a**) Pebble to fine cobble conglomerate with clasts coated by matrix of red mudstone. (**b**, **b**′) Oblique clinoform surface within breccio-conglomeratic body coated by laminated red mudstone. (**c**) Coated clasts within breccio-conglomeratic body interbedded with thin layers of medium to coarse sandstone (arrow). Car key is 4 cm wide. (**d**, **d**′) Graded bedding in breccio-conglomeratic body with basal erosional surface resting on underlying breccio-conglomerate. (**e**, **e**′) Termination of breccio-conglomeratic body at oblique surface with accretion of laminated calcareous red mudstone with offlapping domical structures that is then overlain by layer of cobble conglomerate encrusted by smaller domes. (**f**, **f**′) Laminated calcareous red mudstone with offlapping domical structures truncated by sub-Diabaig Formation unconformity. (**g**) Rounded cobbles of Lewisian rock deposited between domes in laminated calcareous red mudstone forming the nuclei of domical structures in the overlying red calcareous mudstone. Some laminations are subvertical to overhanging (red arrow). (**h**) Broad offlapping domical structures in red calcareous laminated mudstone overlying layer of cobbles. (**i**) Broad domical structures in laminated red calcareous mudstone near top of exposure; it should be noted that the morphology of the internal laminations mimics the external form.

zoned calcite spar. The clotted micrite forms irregular-shaped rounded bodies up to 5–10 mm in size.

- Reticulate micrite: these form a reticulate network of planar to curved micrite bridges with zoned calcite spar-filled pores between them (Figs 8f and 10). These are often broken down into plate-shaped fragments of micrite. The micrite elements often have a preferential vertical alignment (Fig. 8f), corresponding to upright projections in the upper surface of the carbonate body. The micrite is homogeneous and has the same mottled to speckly moderate yellowish orange luminescence as the clotted micrite.

Both types of carbonate bodies sometimes have a laminated fabric that appears to form on the outer surface of the body (e.g. Figs 8e and 10a, b). Internal pores within both clotted and reticulate micrite are lined by scattered crystals of brightly luminescent calcite followed by a phase of pore-filling non-luminescent blocky calcite spar (Figs 9 and 10). A set of sub-parallel microfractures infilled by brightly luminescent zoned calcite often exploit pre-existing crystal boundaries and cross-cut pressure dissolution seams between carbonate bodies (Figs 9a, b and 10a, b). Any remaining porosity is infilled by brightly luminescent calcite cement (e.g. Fig. 10c and d).

Interpretation of logged sections

Clachtoll Formation, Clachtoll, localities 1 and 2

Stewart (2002) interpreted the thickly bedded structureless sandstone that under- and overlies the two logged sections (localities 1 and 2) as a lake basin facies. The two logged sections are interpreted as emergent to very shallow water lake margin facies (Fig. 11a).

The predominance of fine-grained laminated sediment indicates deposition in overall low-energy conditions. The symmetrical bimodal ripples are interpreted as wave ripples, resulting from wind action in shallow water rather than ripples formed in a unidirectional current. Cut and fill structures are interpreted as minor scours, possibly associated with the distal parts of small channels. The convolute and chaotic bedding and the foundering of ripples and cut and fill structures indicate dewatering as a result of deposition on unconsolidated sediment. These were deposited in shallow water, possibly not more than a few centimetres deep at a lake margin. Fine and medium sandstone layers with tabular mudstone clasts may indicate redeposition of desiccated muddy overbank or lake margin sediment during occasional floods. Polygonal fractures infilled by sand indicate desiccation and emergence, and imply deposition in higher parts of the lake margin prone to episodic exposure. The sinuous nature of the fractures suggests that they formed in soft sediment and were compacted.

The stringers of silt- and fine sandstone between low-relief laterally linked domes on mudstone and siltstone bedding planes are interpreted as infills of microchannels possibly not more than a few millimetres deep. This suggests that the domes formed micro-topographic relief and were resistant to erosion, implying that the sediment was bounded by either a microbial mat or a biofilm. The associated polygonal sinuous fractures are interpreted as desiccation fractures and indicate fluctuating water levels in very shallow water. The polygonal network of ridges seen in bedding plane exposures of carbonate sheets are also interpreted as desiccation structures, but the lack of associated fractures suggests that they represent desiccation curls that form when a sediment bounded by a cohesive mat undergoes shrinkage as it dries out (e.g. Shinn 1983).

The steep, sometimes vertical margins of both smooth and cuspate domes suggest that the sediment was bounded and was able

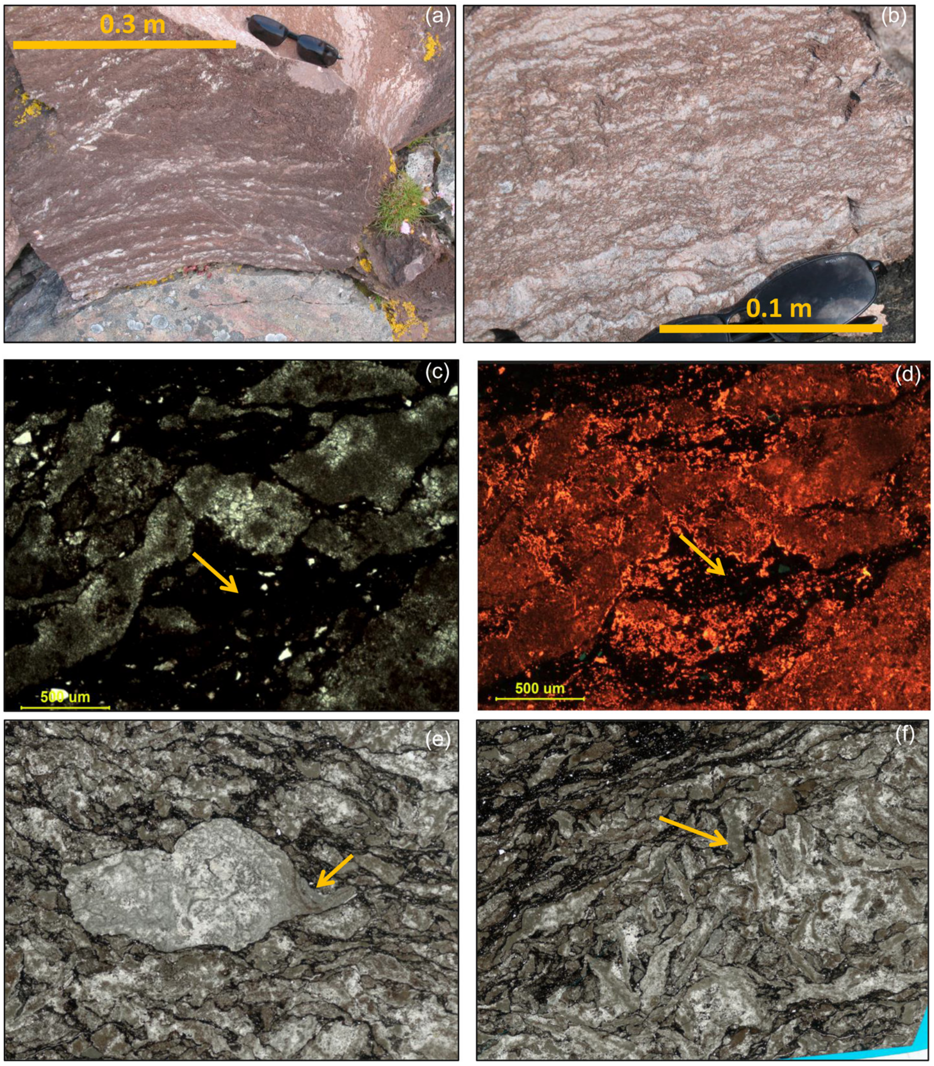

Fig. 8. (**a**, **b**) Larger, irregular carbonate bodies (white) in laminated calcareous red mudstone are concentrated in layers with their long axes parallel to the layering. Interbedded with smaller carbonate bodies with stylolitic concentrations of red mudstone. Poll a'Mhuilt Member, Enard Bay, locality 4. (**c**, **d**) Fragments of moderately luminescent peloidal micrite surrounded by patches of non-luminescent detrital matrix (arrow). Cathodoluminescence–plane-polarized light (CL/ppl) pair. Poll a'Mhuilt Member, Enard Bay, locality 4. (**e**) Large, rounded carbonate body with peloidal texture partly surrounded by laminar micrite structure (arrow). Surrounded by smaller peloidal carbonate bodies and pervasive pressure dissolution seams (dark) wisps. Scanned thin section, field of view 2 cm, Poll a'Mhuilt Member, Enard Bay, locality 4. (**f**) Laminated calcareous red mudstone dominated by tabular clasts of reticulate micrite (arrow) with pervasive pressure dissolution seams (dark wisps). Scanned thin section, field of view 2 cm, Poll a'Mhuilt Member, Enard Bay, locality 4.

to support steep depositional slopes. The onlap of the domes by layered sediment suggests that they were depositional features and the similarity of the form of internal carbonate laminae with their external morphology and the thinning of carbonate layers towards the margins of the domes suggests that that they are constructional features. The general symmetry of the smooth and crinkly domes suggests that they formed in standing or gently agitated water.

Brasier *et al.* (2017, 2019) interpreted the carbonate sheets and domes to be dewatering structures, in some cases modified by desiccation. Although dewatering structures are present in associated sediments, the majority of domical structures are onlapped by undisturbed planar laminated sediment. The smooth domes also have a consistent sub-symmetrical convex-up attitude with sub-parallel tops, bases and internal lamination. Their alternating back-stepping and progradational morphology (e.g. Fig. 4b) cannot be explained by dewatering. Cuspate domes (e.g. Fig. 4c) have flat or gently undulatory bases above which the internal lamination shows a progressive upward tightening of any apparent 'folds'. The carbonate laminae are continuous across these structures with no penetration in the cores of the upright 'folds' that might have been the result of upward injection of fluidized sediment. Further, foundered ripples and convolute lamination in dewatered layers sometimes contain overturned or recumbent folds (e.g. Fig. 3e), geometries that have not been observed in either smooth or cuspate domes. The general convex-up geometry and the outward dip of laminae at the margins of the domical structures are also inconsistent with foundering of unconsolidated sediment and the upward injection of fluidized sediment.

The onlap of smooth and cuspate domes and the similarity of the form of the internal laminae and their external morphology surrounding sediments suggests that they were constructional structures that formed areas of positive depositional relief. The vertical and steep slopes of margins of some domes suggest that the sediment was bounded. The alternating back-stepping and progradational morphology of domes and the alternations between planar and crenulate growth forms (e.g. Fig. 4a) that occur at the same level in adjacent domes indicate a biological origin.

Poll a'Mhuilt Member, Bay of Stoer, locality 3

A depositional model is shown by Figure 11b. Interval 1 is interpreted as a lake margin environment with planar and ripple-bedded sandstone, siltstone and mudstone deposited in an overall low-energy setting in shallow water, probably not more than a few centimetres in depth. Horizons of polygonal fractures represent episodes of desiccation indicating fluctuation of the water level. The acicular and chevron-shaped pseudomorphs are interpreted as evaporite crystals that grew in the sediment, implying concentration of water by evaporation. The tufted carbonate sheets with their consistently flat bases and upward conical projections onlapped by sediment are interpreted as calcified mats in agreement with Upfold (1984) and not as replaced evaporites (Stewart 2002; Brasier 2011) that would have produced more irregular nodular forms. Laterally linked symmetrical domical structures seen on siltstone and mudstone bedding surfaces are associated with desiccation surfaces, suggesting that they formed in very shallow water to emergent

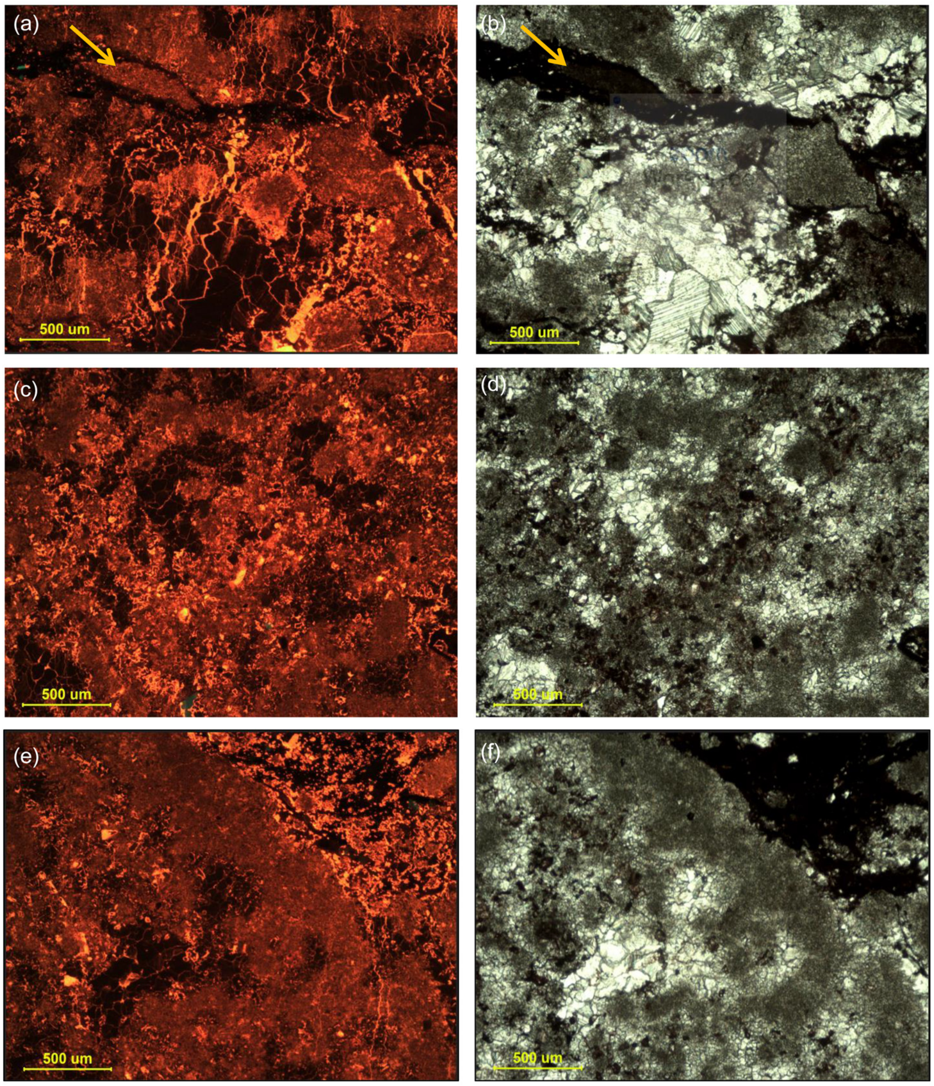

Fig. 9. Poll a'Mhuilt Member, Enard Bay, locality 4. (**a**, **b**) Carbonate body with moderately luminescent peloids cemented by non-luminescent calcite cut by hairline fractures cemented by brightly luminescent calcite. A moderately luminescent lens of micrite is present in the non-luminescent detrital matrix (arrow). CL/ppl pair. Poll a'Mhuilt Member, Enard Bay, locality 4. (**c**, **d**) Moderately luminescent peloidal fabric cemented by non-luminescent calcite. CL/ppl pair. Poll a'Mhuilt Member, Enard Bay, locality 4. (**e**, **f**) Carbonate body with moderately luminescent peloidal fabric cemented by scattered brightly luminescent calcite crystals and non-luminescent calcite spar. Top right, matrix of non-luminescent detrital mudstone and peloidal fragments. CL/ppl pair. Poll a'Mhuilt Member, Enard Bay, locality 4.

conditions in shallow lake margin settings. Their symmetrical, subrounded dome-like structures suggest that these formed by constructional growth that was resistant to erosion. The beds of structureless fine sandstone are interpreted as unconfined mud flows or high-density flows deposited on a lake margin.

The thicker laminated carbonate structures in intervals 2 and 3 are interpreted to have developed by the progressive amalgamation and stacking of individual carbonate mats. The mimicking of external morphology and the offlapping and amalgamation of internal domical structures are interpreted as constructional features. The carbonate unit at the top of interval 2 is interpreted as a biohermal structure that developed in an abandoned channel. The carbonate unit that caps interval 3 is interpreted as a biohermal structure several metres thick and several tens of metres in lateral extent that formed in water several metres deep.

Stewart and Parker (1979) and Parnell *et al.* (2015) interpreted the presence of evaporite pseudomorphs, elevated boron in illite and molybdenum in this section to indicate an evaporitic lacustrine environment. Stüeken *et al.* (2017) proposed a marginal marine setting based on flaser bedding and herringbone cross-stratification with mud drapes; however, bimodal cross-bedding has been found at other localities where it has been interpreted as the result of wave reworking in a lake margin setting. Stüeken *et al.* (2017) also presented geochemical evidence for marine influence in this section based on isotopically enriched molybdenum (+1.19‰ δ^{98}Mo) and the ^{87}Sr/^{86}Sr ratio of 0.707 in carbonate indicating precipitation from mixed freshwater and marine water. The depositional setting is interpreted as a marine-influenced lake margin or part of an estuary.

Poll a'Mhuilt Member, Enard Bay, locality 4

The very coarse clast size, angularity and poorly sorted nature of the breccio-conglomerates and the offlapping geometry with clinoforms suggest that they represent offlapping proximal fan-delta lobes (Fig. 11c). Clinoforms within and at the termination of these bodies are interpreted as the intermediate or final positions of the fan-delta lobe during episodic progradation.

The coated conglomerate is interpreted as a fluvial facies deposited on the topographically flat inner fan area, possibly feeding laterally into a fan delta. The lack of desiccation features within the calcareous red mudstone suggests that the coating formed in a submergent setting. The occurrence of finer-grained sandy layers interbedded with the red mudstone coating is interpreted as periods of lower energy discharge. The calcareous red mudstone is not a concentric oncolitic coating of individual clasts (e.g. Flügel 2004) but is interpreted as a superficial binding of the alluvial surface that formed during periods of non-deposition in an otherwise high-energy setting. Clinoform surfaces were also coated by the red mudstone during periods of fan-lobe inactivity or following abandonment (e.g. Figs 7b and 11c).

The calcareous laminated red mudstone forms a thick coating of abandoned fan-delta lobes forming an offlapping biohermal

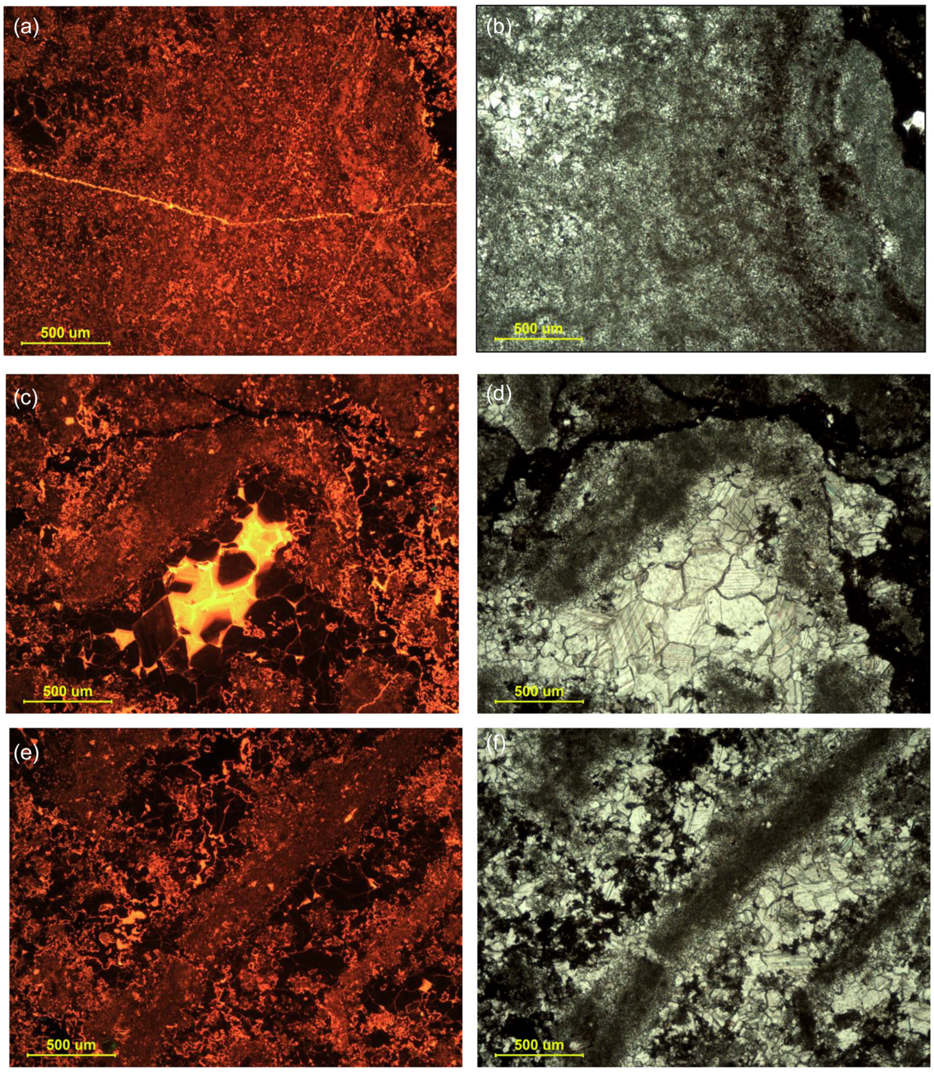

Fig. 10. (**a**, **b**) Reticulate micrite cemented by non-CL calcite passes into curved laminar micrite to the right of image. Moderately luminescent laminar micrite cut by hairline fracture cemented by brightly luminescent calcite. CL/ppl pair. Poll a'Mhuilt Member, Enard Bay, locality 4. (**c**, **d**) Moderately luminescent reticulate micrite cemented by initial patchy brightly luminescent calcite then filled by zoned non- to brightly luminescent calcite. CL/ppl pair. Poll a'Mhuilt Member, Enard Bay, locality 4. (**e**, **f**) Moderately luminescent reticulate micrite cemented by non-luminescent and then brightly luminescent zoned calcite. CL/ppl pair. Poll a'Mhuilt Member, Enard Bay, locality 4.

structure composed of broad overlapping domes. A veneer of rounded cobbles was deposited on the lithified surface of the bioherm with some cobble-sized clasts that settled between domes (Fig. 7g). These clasts were then coated by the laminated calcareous mudstone, some of which was near-vertical to overhanging, to form domical structures centred on the clasts that further expanded to produce a larger structure of numerous broad overlapping domes.

The similarity between the form of carbonate laminae and the external mounded and undulatory geometry of the structure indicates that these domical structures represent a series of constructional structures. The symmetry of the domes suggests that there was no preferential current. These laminated domical structures at Enard Bay are of similar dimensions to domical structures that occur as drapes over cobbles and flat and contorted mats in the Mesoproterozoic Copper Harbor Group described by Elmore (1983), Wilmeth *et al.* (2014) and Fedorchuk *et al.* (2016).

The presence of calcite cement infilling internal pores within the clotted and reticulate micrite indicates that the carbonate bodies were originally porous and the original texture is interpreted as a framestone. The preferential alignment of the reticulate fabric and the presence of laminated micrite at the margins of some carbonate bodies suggest that they may represent biologically mediated production that formed calcified structures. The framestone fabric also suggests that the carbonate bodies were brittle during deposition and were unlikely to survive reworking and transportation. They are therefore unlikely to have been detrital clasts that accumulated on the laminated structures. The laminated calcareous red mudstone is interpreted as a composite biohermal structure that developed by local biologically mediated production of carbonate and binding and stabilization of sediment represented by the red mudstone. The bioherms nucleated over the terminations of fan lobes and adjacent parts of the submerged Lewisian surface at a lake margin. The thickness of the structure suggests that the lake was several metres deep at this point (Fig. 11c).

Discussion

Stromatolitic origin of the laminated carbonate structures

Facies analysis of associated sediments indicates that the laminated carbonate structures formed in water depths ranging from a few millimetres to several metres deep in settings that included very shallow water freshwater and marine-influenced lake margins that were episodically emergent, abandoned channels and draping the terminations of fan-delta lobes that prograded into a lake. Stewart (2002) and Brasier *et al.* (2017, p. 133; 2019, p. 314) considered the laminated carbonate structures to be of clastic origin incorporating detrital clasts of metamorphic carbonates but did not expand on possible mechanisms; however, the following observations point to biological accretion of these structures:

- onlap of sediment indicates that the domes formed depositional structures with topographic relief (e.g. Fig. 4a and b);

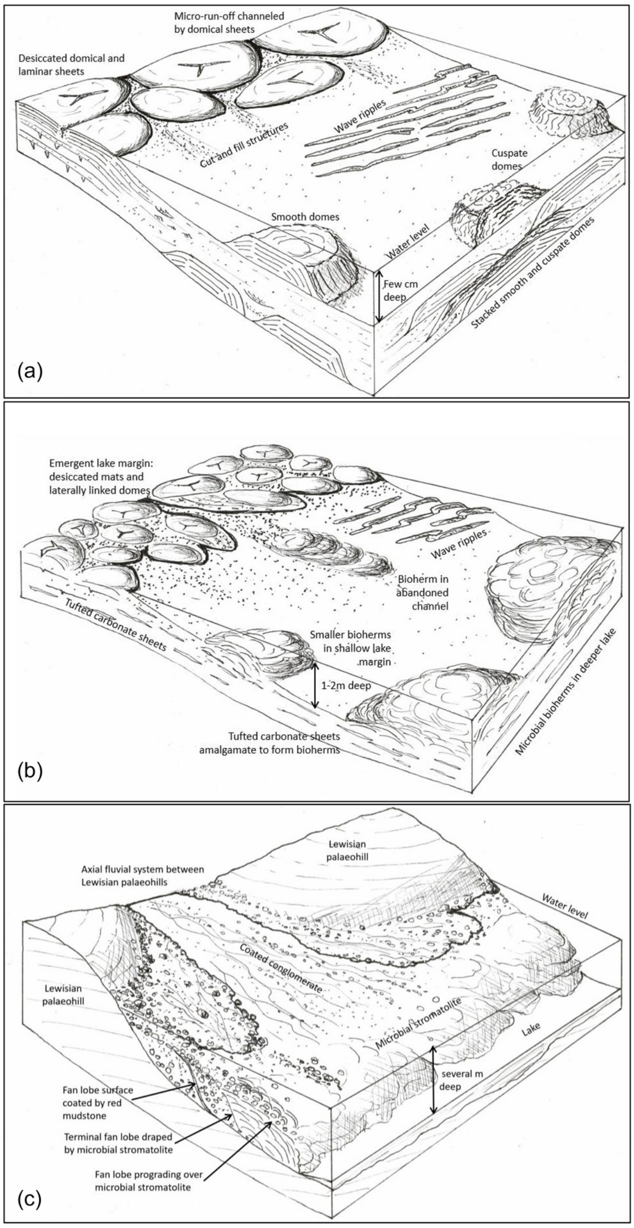

Fig. 11. (**a**) Lake margin depositional setting of the Clachtoll Formation at localities 1 and 2. Laminar sheets for low-relief laterally linked domes in partly emergent lake margin with runoff channels between the domes. Smooth and crinkly domes form in deeper, submerged parts of the lake margin. (**b**) Depositional model for basal part of the Poll a'Mhuilt Member, Bay of Stoer, locality 3. Laterally linked low relief symmetrical non-calcareous domical structures with individual laminar carbonate sheets and interbedded desiccation surfaces are interpreted as lake margin with episodic exposure. Sinuous-crested ripples with individual and stacked carbonate sheets represent shallow submerged lake margins. Larger biohermal structures develop in deeper lake and in abandoned channels. (**c**) Depositional model for the Poll a'Mhuilt Member, Enard Bay, locality 4. Locally sourced proximal fluvial breccio-conglomerates accumulate as axial fluvial systems between palaeohills in the Lewisian surface. These terminate as a number of fan-delta lobes prograding into a lake. Coating of the fluvial surface and fan-delta lobe terminations by red mudstone took place during pauses in runoff. Large biohermal structures develop over the terminations of fan-delta lobes and the submerged Lewisian surface in the lake margin setting.

- mimicking of internal geometry of the laminae with external form indicates that they represent constructional features (e.g. Figs 4b, 6g, h and 7h, i);
- progressive offlapping morphology and progressive expansion and amalgamation of domes forms larger structures (e.g. Figs 6h and 7g–i);
- back-stepping alternates with progradational domes (e.g. Fig. 4b);
- broad smooth domes alternate with smaller isolated domes (e.g. Fig. 4b);
- carbonate laminae within domes often show morphological variations throughout the development of an individual dome that can sometimes be matched between adjacent domes, suggesting that they may have been subject to external environmental changes (e.g. Fig. 4a).

Fedorchuk *et al.* (2016) outlined further criteria for the possible biogenic origin of fluvio-lacustrine stromatolites from the Mesoproterozoic Copper Harbor Conglomerate in Michigan. They included evidence for sediment binding such as crinkly carbonate fabric that traps and preserves detrital grains beyond their natural angle of repose. The crinkly carbonate fabric forming cuspate domes at Clachtoll Bay shows upward projections with steep, sometimes subvertical sides that include trapped detrital grains (e.g. Fig. 4c). Smooth domes and biohermal structures also have some steep-sided to subvertical and overhanging margins (e.g. Figs 4a and 6g) that require a binding mechanism to support such slopes. Smooth domes are made up of carbonate microspar laminae alternating with mudstone and siltstone layers suggest that binding of detrital sediment as well as carbonate precipitation is required for the formation of these domes (e.g. Fig. 4a). Fedorchuk *et al.* (2016) also mentioned asymmetrical growth in response to light and the presence of fenestrae resulting from the photosynthetic production of O_2 as indicators of biogenesis, but these features were not observed.

Carbonate fabrics described here include microspar and clotted and reticulate textures; the latter two forming a framestone texture were regarded as biogenic indicators by Fedorchuk *et al.* (2016). In contrast, microfabrics such as radial fibrous calcite fans, radiaxial fibrous and fascicular optic calcite or microfabrics characteristic of carbonate cement resulting from abiogenic inorganic or physico-chemical precipitation were not observed (e.g. Flügel 2004; Bosence *et al.* 2015; Fedorchuk *et al.* 2016). Kah and Bartley (2021) recognized a range of microfabrics in Mesoproterozoic carbonates and distinguished tufted, pustular and irregular micritic laminae, equivalent to the tufted, clotted and reticulate fabrics described here, as associated with microbial fabrics often associated with stromatolites. Mattes and Conway Morris (1990), Le Ber *et al.* (2015) and Mettraux *et al.* (2015) also described microspar laminae and clotted and reticulate micrite from Neoproterozoic microbial stromatolites and thrombolites from Oman that resemble the textures described from the Stoer Group. A further point of similarity is that standard and CL petrographic studies by the above-cited researchers showed that the clotted and reticulate micrite masses form a framework cemented by calcite spar or with preserved porosity. Other examples of clotted and reticulate micrite have been described from microbial stromatolites and thrombolites from the Eocene Green River Formation, the recent Great Salt Lake in Utah and Lake Thetis in western Australia (Grey *et al.* 1990; Chidsey *et al.* 2015; Baskin *et al.* 2022).

The carbonate component is interpreted to form a template around biofilms formed by filamentous and coccoid cyanobacteria or nucleated on extracellular polymeric substances by the interaction of microbial metabolism with supersaturated carbonate pore fluid (e.g. Riding 2002, 2008; Bosence *et al.* 2015). The main mechanisms of precipitation are interpreted as biologically induced calcification and biologically influenced calcification (Dupraz *et al.* 2009). Reid *et al.* (2000) and Lan *et al.* (2020) suggested that modern and ancient marine stromatolites represent a dynamic balance between sedimentation and the growth and intermittent lithification of biofilms formed by filamentous and coccoid cyanobacteria. It is possible that some of the structures in the Stoer Group may have formed by a combination of calcifying and non-calcifying microbial mats. The variations of microfabric may also reflect varying pore fluid chemistry or differing microbial assemblages. Geochemical evidence for possible microbial activity during deposition of the Stoer Group was also provided by Parnell *et al.* (2010), who attributed S isotope fractionation to microbial sulfate reduction, and Spinks *et al.* (2010), who identified vanadium-rich micas at the core of reduction spots in shales as a proxy for microbial activity.

Brasier *et al.* (2017, p. 133; 2019, p. 314) also proposed that the carbonate bodies in the Enard Bay bioherm represent detrital clasts reworked from metamorphic carbonates. However, the carbonate microfabric is characteristic of microbially mediated precipitates and does not display annealed textures, which would be expected in reworked metamorphic carbonates. The clumped isotope temperature of 160°C obtained by Brasier *et al.* (2019) indicates that these carbonates have not reached the onset of low-grade metamorphism defined as 200–250°C (Immenhauser 2022) but is more likely to reflect later Mesoproterozoic burial (Stewart 2002) and not an inherited metamorphic temperature.

Sediment surface textures and their relationship to stromatolites

The laterally linked domes on mudstone and siltstone bedding planes (e.g. Figs 3h and 6b) may provide evidence of sediment stabilization by microbial mats or biofilms that support the domical topography and provide resistance to erosion with the preservation of sediment in microchannels between domes. Desiccated carbonate sheets showing polygonal ridges (Fig. 3g) are also interpreted as indicators of sediment binding. The coated conglomerate also shows evidence of sediment binding of sand layers between pebbles, fluvial surfaces and inclined surfaces of the intermediate or abandonment surfaces of fan-delta lobes. The origin of these features is uncertain but has been attributed to microbially induced sedimentary structures (e.g. Prave 2002; Brasier *et al.* 2017, 2019; McMahon and Davies 2018), implying that they result from the biostabilization of sediment by the presence of biofilms and microbial mats as defined by Noffke (2009). However, the biological significance of these structures has not been conclusively proven and the term sediment surface texture is used instead (e.g. Davies *et al.* 2016).

The difference between the development of sediment surface texture as opposed to stromatolites may have been the level of carbonate saturation of the groundwater and surface water. Microbial communities may have been able to fix carbonate only in porewater that was sufficiently supersaturated with calcium carbonate. An alternative explanation is that sediment surface textures were formed by non-calcifying microbial communities whereas stromatolites represent a differing assemblage of microbial species that were able to calcify. Grey *et al.* (1990), Chidsey *et al.* (2015) and Baskin *et al.* (2022) described modern saline lakes including Lake Thetis in Western Australia and the Great Salt Lake in Utah that are host to a wide range of microbial communities restricted to differing sub-environments, each giving rise to a range of sediment surface textures and stromatolites.

Origin and nature of depositional and early diagenetic pore fluids

The supply of dissolved sulfate and carbonate is a prerequisite to support any possible microbial metabolism and biologically mediated calcification. This section addresses the nature and possible origins of depositional and early diagenetic pore fluids during deposition of the Stoer Group.

Wacey *et al.* (2017) showed that walls of microfossils extracted from the Stoer Group have been pyritized, suggesting the presence of a sulfate-rich, phosphate-poor pore fluid. Parnell *et al.* (2014) described early diagenetic greenockite in the Poll a'Mhuilt Member at the Bay of Stoer. Formation of greenockite requires an anoxic pore fluid enriched in cadmium, suggesting that the low partial pressure of oxygen in the Precambrian atmosphere was insufficient to have produced near-surface oxic diagenesis (Dyrssen 1988; Parnell *et al.* 2014). Wacey *et al.* (2014, 2017) suggested that there was sufficient partial pressure of oxygen in the atmosphere to cause oxidative weathering of sulfides; however, local conditions, such as high rates of erosion or deposition, may have allowed transport and preservation of detrital sulfides and magnetite (e.g. Stewart 1991, 2002; Reinhard *et al.* 2009). Potential sources of sulfate in wholly freshwater environments may have been by oxidative weathering of detrital and *in situ* sulfides in the Lewisian (e.g. Jones *et al.* 1987; Strachan *et al.* 2012; Park 2022). Dissolved sulfate in the basal Poll a'Mhuilt Member at the Bay of Stoer may have been sourced additionally from marine water.

Parnell *et al.* (2014) indicated that groundwater during deposition of the Stoer Group was carbonate-rich and suggested that early oxidation of organic matter was a possible source of carbonate. Brasier *et al.* (2019), using Raman spectroscopy, showed that the Stoer Group contains kerogenous organic carbon and externally sourced detrital graphite. Shales, such as those of the Poll a'Mhuilt Member with an average total organic carbon content of 0.24–0.37 wt%, may have provided the required organic matter during deposition (Stewart 2002; Stüeken *et al.* 2017). Cerling (1994) emphasized the importance of arid weathering of basic and ultrabasic volcanic rocks to create high carbonate alkalinity in present-day African Rift Valley lakes. Although there are no volcanic rocks in the hinterland of the Stoer Group, semi-arid weathering of basic and ultrabasic Scourian dykes may have generated carbonate-rich groundwater. Marine water may also have provided a source of dissolved carbonate either directly in marginal marine settings or in marine–meteoric mixing zones. Bartley and Kah (2004) estimated that Proterozoic marine water contained between two and 10 times more dissolved inorganic carbon compared with present-day ocean water, which would have sustained elevated carbonate saturation.

Conclusions

Smooth and cuspate domes and biohermal structures composed of laminated carbonate and fine siliciclastic laminae occur in the Mesoproterozoic Stoer Group in submerged and desiccated lake margins and at the termination of fan-delta lobes where they prograded into lakes. Evidence for the biological origin of these structures includes the following:

- steep, subvertical and locally overhanging margins of domes and bioherms indicating sediment binding;
- mimicking of internal geometry with external form indicating that these structures represent constructional features;
- alternation of back-stepping with progradational morphological forms;
- progressive offlapping morphology and progressive expansion and amalgamation of domes to form larger structures;
- microspar, clotted and reticulate carbonate fabrics forming a framestone texture that resembles documented microbial carbonate fabrics.

The smooth and cuspate domes and biohermal structures fulfil the definition by Riding (1999, 2011*a*, *b*) of microbial stromatolites as

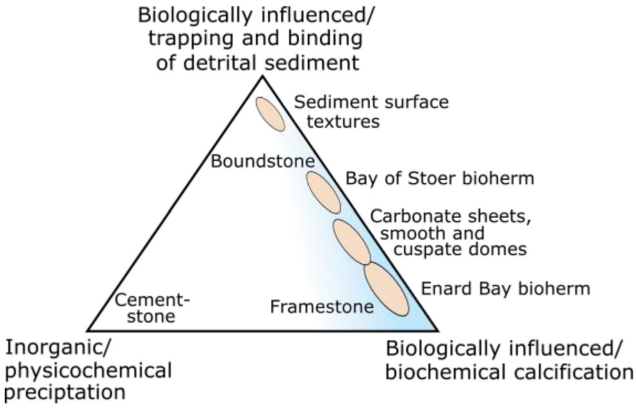

Fig. 12. Triangular diagram showing structures identified in this study in terms of depositional fabric and the processes of microbialite formation. Source: modified from Burne and Moore (1987), Riding (1977) and Bosence *et al.* (2015).

'macroscopically layered authigenic microbial sediments with or without abiogenic precipitates' and thus represent the oldest microbial stromatolites in the British Isles.

The laminated carbonate structures are associated with sediment surface textures including laterally linked domes on mudstone bedding planes, desiccated carbonate sheets and coated conglomerates. These also imply sediment binding; however, it is not clear to what extent any biological influence was involved. Sediment surface textures may have developed instead of stromatolites because of the level of carbonate saturation of the groundwater and surface water. Microbial communities may have been able to fix carbonate only in porewater that was sufficiently supersaturated with calcium carbonate. Alternatively, differing assemblages of microbial species may have been responsible for sediment surface textures and stromatolites.

Figure 12 shows the laminated carbonate structures and sediment surface textures in terms of their depositional fabric on the triangular diagram showing the inferred processes of microbialite formation (after Riding 1977; Burne and Moore 1987; Bosence *et al.* 2015). The smooth and cuspate domes and the Bay of Stoer biohermal stromatolites contain layers of detrital sediment alternating with microbially mediated carbonate layers and represent structures with biologically influenced carbonate precipitation combined with trapping and binding of detrital sediment.

Dissolved sulfate was supplied by weathering of detrital and *in situ* sulfides derived from the Lewisian hinterland, and carbonate may have been supplied by semi-arid weathering of basic and ultrabasic Scourian dykes. Marine–meteoric mixing zones are an additional possible source of dissolved sulfate and carbonate.

Scientific editing by Alex Dunhill

Acknowledgements I thank editor A. Dunhill and reviewers W. McMahon and P. Wright for their time and comments; also J. Garland and A. Horbury of Cambridge Carbonates Ltd, who allowed use of their cathodoluminoscope. This paper is dedicated to my Leeds University mentors H. Clemmey, M. Leeder and the late M. Coward.

Author contributions **PG**: formal analysis (lead), writing – original draft (lead)

Funding This study is self-funded.

Competing interests The author declares that they have no known competing financial interests or personal relationships that could have appeared to influence the work reported in this paper.

Data availability The only permanent data generated by this study are a set of thin sections. I am happy to make these available to interested parties.

References

Amor, K., Hesselbo, S.P., Porcelli, D., Thackrey, S. and Parnell, S. 2008. A Precambrian proximal ejecta blanket from Scotland. *Geology*, **36**, 303–306, https://doi.org/10.1130/G24454A.1

Bartley, J.K. and Kah, L.C. 2004. Marine carbon reservoir, C_{org}–C_{carb} coupling and the Proterozoic carbon isotopic record. *Geology*, **32**, 129–132, https://doi.org/10.1130/G19939.1

Baskin, R.L., Della Porta, G. and Wright, V.P. 2022. Characteristics and controls on the distribution of sublittoral microbialite bioherms in Great Salt Lake, Utah: implications for understanding microbialite development. *Depositional Record*, **8**, 39–66, https://doi.org/10.1002/dep2.159

Bosence, D.W.J., Gibbons, K.A., Le Heron, D.P., Morgan, W.A., Pritchard, T. and Vining, B. 2015. Microbial carbonates in space and time: introduction. *Geological Society, London, Special Publications*, **418**, 1–15, https://doi.org/10.1144/SP418.14

Brasier, A.T. 2011. Search for travertines, calcretes and speleothems in deep time: processes, appearances, predictions and the impact of plants. *Earth-Science Reviews*, **104**, 213–239, https://doi.org/10.1016/j.earscirev.2010.10.007

Brasier, A.T., Culwick, T., Battison, L., Callow, R.H.T. and Brasier, M.D. 2017. Evaluating evidence from the Torridonian Supergroup (Scotland, UK) for eukaryotic life on land in the Proterozoic. *Geological Society, London, Special Publications*, **448**, 121–144, https://doi.org/10.1144/SP448.13

Brasier, A.T., Dennis, P.F. *et al.* 2019. Detecting ancient life: investigating the nature of possible stromatolites and associated calcite from a one-billion-year-old lake. *Precambrian Research*, **328**, 309–320, https://doi.org/10.1016/j.precamres.2019.04.025

Burne, R.V. and Moore, L.S. 1987. Microbialites: organosedimentary deposits of benthic microbial communities. *Palaios*, **2**, 241–254, https://doi.org/10.2307/3514674

Cerling, T.E. 1994. Chemistry of closed lake basin waters: a comparison between African Rift Valley- and some central North American rivers and lakes. *In*: Gierlowski-Kordesch, E.H. and Kelts, K. (eds) *The Global Geological Record of Lake Basins*, **1**. University Press, Cambridge, 29–30.

Chidsey, T.C., Jr, Vanden Berg, M.D. and Eby, D.E. 2015. Petrography and characterization of microbial carbonates and associated facies from modern Great Salt Lake and Uinta Basin's Eocene Green River Formation in Utah, USA. *Geological Society, London, Special Publications*, **418**, 261–286, https://doi.org/10.1016/j.earscirev.2016.01.005

Davies, N.S., Liu, A.G., Gibling, M.R. and Miller, R.F. 2016. Resolving MISS conceptions and misconceptions: a geological approach to sedimentary surface textures generated by microbial and abiotic processes. *Earth-Science Reviews*, **154**, 210–246, https://doi.org/10.1016/j.earscirev.2016.01.005

Dupraz, C., Reid, R.P., Braissant, O., Decho, A.W., Norman, R.S. and Visscher, P.T. 2009. Processes of carbonate precipitation in modern microbial mats. *Earth-Science Reviews*, **96**, 141, https://doi.org/10.1016/j.earscirev.2008.10.005

Dyrssen, D. 1988. Sulphide complexation in surface sea water. *Marine Chemistry*, **24**, 143–153, https://doi.org/10.1016/0304-4203(88)90045-X

Elmore, R.D. 1983. Precambrian non-marine stromatolites in alluvial fan deposit, the Copper Harbor Conglomerate, upper Michigan. *Sedimentology*, **30**, 829–842, https://doi.org/10.1111/j.1365-3091.1983.tb00713.x

Fedorchuk, N.D., Dornbos, S.Q., Corsetti, F.A., Isbell, J.L., Petryshyn, V.A., Bowles, J.A. and Wilmeth, D.T. 2016. Early non-marine life: evaluating the biogenicity of Mesoproterozoic fluvio-lacustrine stromatolites. *Precambrian Research*, **275**, 105–118, https://doi.org/10.1016/j.precamres.2016.01.015

Flügel, E. 2004. *Microfacies of Carbonate Rocks; Analysis, Interpretation and Application*. Springer, Berlin.

Goodenough, K.M. and Krabbendam, M. 2011. *A Geological Excursion Guide to the North-West Highlands of Scotland*. National Museums of Scotland.

Gracie, A.J. and Stewart, A.D. 1967. Torridonian sediments at Enard Bay, Ross-shire. *Scottish Journal of Geology*, **3**, 181–194, https://doi.org/10.1144/sjg03020181

Grey, K., Moore, L.S., Burne, R.V., Pierson, B.K. and Bauld, J. 1990. Lake Thetis, Western Australia: an example of saline lake sedimentation dominated by benthic microbial processes. *Australian Journal of Marine and Freshwater Research*, **41**, 275–300, https://doi.org/10.1071/MF9900275

Ielpi, A., Ventra, D. and Ghinassi, M. 2016. Deeply-channeled Precambrian rivers: remote sensing and outcrop evidence from the 1.2 Ga Stoer Group of NW Scotland. *Precambrian Research*, **281**, 291–311, https://doi.org/10.1016/j.precamres.2016.06.004

Immenhauser, A. 2022. On the delineation of the carbonate burial realm. *Depositional Record*, **8**, 524–574, https://doi.org/10.1002/dep2.173

Jones, E.M., Rice, C.M. and Tweedie, J.R. 1987. Lower Proterozoic stratiform sulphide deposits in Loch Maree Group, Gairloch, North West Scotland. *Transactions of the Institution of Mining and Metallurgy*, **96**, B128–B140.

Kah, L.C. and Bartley, J.K. 2021. Carbonate fabric diversity and environmental heterogeneity in the late Mesoproterozoic era. *Geological Magazine*, **159**, 220–246, https://doi.org/10.1017/S0016756812100406

Killingback, Z., Holdsworth, R.E., Walker, R.J., Nielsen, S., Dempsey, E. and Hardman, K. 2021. A bigger splat: the catastrophic geology of a 1.2-b.y.-old terrestrial megaclast, northwest Scotland. *Geology*, **49**, 180–184, https://doi.org/10.1130/G48079.1

Lan, Z., Zhang, S., Tucker, M.E., Li, Z. and Zhao, Z. 2020. Evidence for microbes in Neoproterozoic stromatolites. *Sedimentary Geology*, **398**, https://doi.org/10.1016/j.sedgeo.2020.105589

Le Ber, E., Le Heron, D.P. and Oxtoby, N.H. 2015. Influence of microbial framework on Cryogenian microbial facies, Rasthof Formation, Namibia. *Geological Society, London, Special Publications*, **418**, 111–122, https://doi.org/10.1144/SP418.7

Mattes, B.W. and Conway Morris, S. 1990. Carbonate/evaporite deposition in the late Precambrian–early Cambrian Ara Formation of southern Oman. *Geological Society, London, Special Publications*, **49**, 617–636, https://doi.org/10.1144/GSL.SP.1992.049.01.37

McMahon, W.J. and Davies, N.S. 2018. High energy flood events recorded in the Mesoproterozoic Meall Dearg Formation, NW Scotland; their recognition and implications for the study of pre-vegetation alluvium. *Journal of the Geological Society, London*, **175**, 13–32, https://doi.org/10.1144/jgs2017-012

Mettraux, M., Homewood, P. *et al.* 2015. Microbial communities and their primary to early diagenetic mineral phases; the record from Neoproterozoic microbialites of Qarn Alam, Oman. *Geological Society, London, Special Publications*, **418**, 123–154, https://doi.org/10.1144/SP418.5

Noffke, N. 2009. The criteria for the biogenicity of microbially induced sedimentary structures (MISS) in Archaean and younger sandy deposits. *Earth-Science Reviews*, **96**, 173–180, https://doi.org/10.1016/j.earscirev.2008.08.002

Park, G. 2022. *The Lewisian, Britain's Oldest Rocks*. Liverpool University Press.

Parnell, J., Boyce, A.J., Mark, D., Bowden, S. and Spinks, S. 2010. Early oxygenation of the terrestrial environment during the Mesoproterozoic. *Nature*, **468**, 290–293, https://doi.org/10.1038/nature09538

Parnell, J., Mark, D., Fallick, A.E., Boyce, A.J. and Thackery, S. 2011. The age of the Mesoproterozoic Stoer Group sedimentary and impact deposits, NE Scotland. *Journal of the Geological Society, London*, **168**, 349–358, https://doi.org/10.1144/0016-76492010-099

Parnell, J., Still, J., Spinks, S., Thayalan, W. and Bowden, S. 2014. Cadmium sulphide in a Mesoproterozoic terrestrial environment. *Mineralogical Magazine*, **78**, 47–54, https://doi.org/10.1180/minmag.2014.078.1.04

Parnell, J., Spinks, S., Still, J., Andrews, S., Thayalan, W. and Bowden, S. 2015. High molybdenum availability for evolution in a Mesoproterozoic lacustrine environment. *Nature Communications*, **6**, https://doi.org/10.1038/ncomms7996

Prave, A.R. 2002. Life on land in the Proterozoic: evidence from the Torridonian rocks of northwest Scotland. *Geology*, **30**, 811–814, https://doi.org/10.1130/0091-7613(2002)030<0811:LOLITP>2.0.CO;2

Reid, R.P., Visscher, P.T. *et al.* 2000. The role of microbes in accretion, lamination and early lithification of modern marine stromatolites. *Nature*, **406**, 989–992, https://doi.org/10.1038/35023158

Reinhard, C.T., Raiswell, R., Scott, C., Anbar, A.D. and Lyons, T.W. 2009. A late Archaean sulphidic sea stimulated by early oxidative weathering of the continents. *Science*, **326**, 713–716, https://doi.org/10.1126/science.1176711

Riding, R. 1977. Skeletal stromatolites. *In*: Flügel, E. (ed.) *Fossil Algae Recent Results and Developments*. Springer, Berlin, 57–60.

Riding, R. 1999. The term stromatolite: towards an essential definition. *Lethaia*, **32**, 321–330, https://doi.org/10.1111/j.1502-3931.1999.tb00550.x

Riding, R. 2002. Microbial carbonates: the geological record of calcified bacterial–algal mats and biofilms. *Sedimentology*, **47**, 179–214, https://doi.org/10.1046/j.1365-3091.2000.00003.x

Riding, R. 2008. Abiogenic, microbial and hybrid authigenic carbonate crusts: components of Precambrian stromatolites. *Geologica Croatica*, **61**, 73–103, https://doi.org/10.4154/gc.2008.10

Riding, R. 2011a. Nature of stromatolites: 3500 myrs of history and a century of research. *Lecture Notes in Earth Sciences*, **131**, https://doi.org/10.1007/978-3-642-10415-2_3

Riding, R. 2011b. The term stromatolite: towards an essential definition. *Lecture Notes in Earth Sciences*, **131**, https://doi.org/10.1007/978-3-642-10415-2_3

Shinn, E.A. 1983. Tidal flat environment. *AAPG Memoirs*, **33**, 171–210.

Spinks, G., Parnell, J. and Bowden, S.A. 2010. Reduction spots in the Mesoproterozoic age: implications for the life in the early terrestrial record. *International Journal of Astrobiology*, **9**, 209–216, https://doi.org/10.1017/S1473550410000273

Stewart, A.D. 1991. Geochemistry, provenance and palaeoclimate of the Upper Proterozoic Stoer Group in Scotland. *Scottish Journal of Geology*, **26**, 89–97, https://doi.org/10.1144/sjg26020089

Stewart, A.D. 2002. *The Later Proterozoic Torridonian Rocks of Scotland: Their Sedimentology, Geochemistry and Origin*. Geological Society, London, Memoirs, **24**.

Stewart, A.D. and Parker, A. 1979. Palaeosalinity and environmental interpretations of red beds from the late Precambrian ('Torridonian') of Scotland. *Sedimentary Geology*, **22**, 229–241, https://doi.org/10.1016/0037-0738(79)90054-X

Strachan, R.A., Holdsworth, R.E. and Prave, A.R. 2012. Proterozoic sedimentation, orogenesis and magmatism on the Laurentian Craton (2500–750 Ma). *In*: Woodcock, N.H. and Strachan, R.A. (eds) *Geological History of the British Isles*. Wiley–Blackwell, 54–75.

Stüeken, E.E., Bellefroid, E.J., Prave, A., Asael, D., Planavsky, N.J. and Lyons, T.W. 2017. Not so marine? Revisiting the Stoer Group and the Mesoproterozoic biosphere. *Geochemical Perspectives Letters*, **3**, 221–229, https://doi.org/10.7185/geochemlet.1725

Turnbull, M.J.M., Whitehouse, M.J. and Moorbath, S. 1996. New isotopic age determinations for the Torridonian, NW Scotland. *Journal of the Geological Society, London*, **153**, 955–964, https://doi.org/10.1144/gsjgs.153.6.0955

Upfold, R.L. 1984. Tufted microbial (cyanobacterial) mats from the Proterozoic Stoer Group, Scotland. *Geological Magazine*, **121**, 351–355, https://doi.org/10.1017/S0016756800029253

Valenza, J.M., Ganti, V., Whittaker, A.C. and Lamb, M.P. 2019. Pre-vegetation, single thread rivers sustained by cohesive, fine-grained bank sediments: Mesoproterozoic Stoer Group, NW Scotland. *Geophysical Research Letters*, **50**, e2023GL104379, https://doi.org/10.1029/2023GL104379

Wacey, D., Saunders, M., Roberts, M., Menon, S., Kong, C., Strother, P. and Brasier, M.D. 2014. Enhanced cellular preservation by clay minerals in 1 billion-year-old lakes. *Scientific Reports*, **4**, https://doi.org/10.1038/srep05841

Wacey, D., Batisson, L., Garwood, R.J., Hickman-Lewis, K. and Brasier M.D. 2017. Advanced analytical techniques for studying the morphology and chemistry of Proterozoic microfossils. *Geological Society, London, Special Publications*, **448**, 81–104, https://doi.org/10.1144/SP448.4

Wilmeth, D.T., Dornbos, S.Q., Isbell, J. and Czaja, A.D. 2014. Putative domal microbial structures in fluvial siliciclastic facies of the Mesoproterozoic (1.09 Ga) Copper Harbor Conglomerate, Upper Peninsula of Michigan, USA. *Geobiology*, **12**, 99–108, https://doi.org/10.1111/gbi.12071